Articles in PresS. J Neurophysiol (May 19, 2010). doi:10.1152/jn.00034.2010

GAIN OF FUNCTION IN FHM-1 $Ca_V2.1$ KNOCK-IN MICE IS RELATED TO THE SHAPE OF THE ACTION POTENTIAL

Carlota González Inchauspe [1], Francisco J. Urbano [1], Mariano N. Di Guilmi [1], Ian D. Forsythe [2], Michel D. Ferrari [3], Arn M.J.M. van den Maagdenberg [3,4], and Osvaldo D. Uchitel [1]

[1]*Instituto de Fisiología, Biología molecular y Neurociencias. CONICET. Departamento de Fisiología, Biología Molecular y Celular, Facultad de Ciencias Exactas y Naturales, Universidad de Buenos Aires, Argentina.*

[2]*Neurotoxicity at the Synaptic Interface, MRC Toxicology Unit, University of Leicester, LE1 9HN. UK. Departments of* [3] *Neurology,* [4]*Human Genetics, Leiden University Medical Centre, P.O. Box 9600, 2300 RC Leiden, The Netherlands.*

Abbreviated title: $Ca_V2.1$ channels in a hemiplegic migraine mouse model

Correspondence should be addressed to Dr. O.D. Uchitel,
E-mail: odu@fbmc.fcen.uba.ar
Laboratorio de Fisiología y Biología Molecular, Instituto de Fisiología, Biología Molecular y Neurociencias (LFBM-IFIBYNE), UBA-CONICET, Intendente Guiraldes 2670, pabellón 2, piso 2, Ciudad Universitaria, C1428BGA-Buenos Aires, Argentina.
FAX : (+54-11) 4576 3321

Abstract

Familial hemiplegic migraine type-1 (FHM1) is caused by missense mutations in the *CACNA1A* gene that encodes the α_{1A} pore-forming subunit of $Ca_V2.1$ Ca^{2+} channels. We used knock-in (KI) transgenic mice harbouring the pathogenic FHM-1 mutation R192Q to study neurotransmission at the calyx of Held synapse and cortical layer 2/3 pyramidal cells (PCs). Using whole cell patch clamp recordings in brainstem slices we confirmed that KI $Ca_V2.1$ Ca^{2+} channels activated at more hyperpolarizing potentials. However, calyceal presynaptic calcium currents (I_{pCa}) evoked by presynaptic action potentials (APs) were similar in amplitude, kinetic parameters and neurotransmitter release.

$Ca_V2.1$ Ca^{2+} channels in cortical layer 2/3 PCs from KI mice also showed a negative shift in their activation voltage. PCs had APs with longer durations and smaller amplitudes than the calyx of Held. AP evoked Ca^{2+} currents (I_{Ca}) from PCs were larger in KI compared to WT mice. In contrast, when I_{Ca} were evoked in PCs by calyx of Held AP waveforms, we observed no amplitude differences between WT and KI mice. In the same way, Ca^{2+} currents evoked at the presynaptic terminals (I_{pCa}) of the calyx of Held by the AP waveforms of the PCs had larger amplitudes in R192Q KI mice that in WT. These results suggest that longer time courses of pyramidal APs were a key factor for the expression of a synaptic gain of function in the KI mice. In addition, our results indicate that consequences of FHM1 mutations might vary according to the shape of APs in charge of triggering synaptic transmission (neurons in the calyx of Held vs. excitatory/inhibitory neurons in the cortex), adding to the complexity of the pathophysiology of migraine.

Key-words: knock-in mice, $Ca_V2.1$ channels, migraine mutation, calyx of Held, cortical pyramidal cells.

Introduction

Transmitter release at central synapses is triggered by Ca^{2+} influx through multiple voltage–gated Ca^{2+} channels (VGCCs) subtypes but increasingly relies on $Ca_V2.1$ (P/Q-type) Ca^{2+} channels with maturation (Iwasaki *et al*. 1998, 2000). Familial hemiplegic migraine type-1 (FHM1) is caused by missense mutations in the *CACNA1A* gene that encodes the α_{1A} subunit of $Ca_V2.1$ Ca^{2+} channels. Typical migraine attacks in FHM patients are associated with transient hemiparesis and are a useful model to study pathogenic mechanisms of the common forms of migraine (Ferrari *et. al*. 2008). Biophysical analysis of FHM-1 Ca^{2+} channel dysfunction in heterologus systems is controversial as both loss-of-function and gain-of-function phenotypes have been reported (Barrett *et al*. 2005; Cao and Tsien, 2005; Hans *et al*. 1999; Kraus *et al*. 1998, 2000; Tottene *et al*. 2002). However, analysis of single-channel properties of human $Ca_V2.1$ channels carrying FHM-1 mutations revealed a consistent increase in channel open probability and Ca^{2+} influx at negative voltages, mainly due to a negative shift in channel activation (Tottene *et al*. 2002, 2005). A *knock-in* (KI) migraine mouse model carrying the human FHM-1 R192Q mutation was generated and exhibits several gain-of-function effects, including a negative shift in $Ca_V2.1$ channel activation in cerebellar granule cells, increased synaptic transmission at the neuromuscular junction and increased susceptibility to cortical spreading depression (CSD) (van den Maagdenberg *et al.* 2004), a likely mechanism of the migraine aura (Lauritzen, 1994). Using microcultures and brain slices from FHM-1 mice, Tottene *et al*. (2009) have recently shown increased probability of glutamate release at cortical layer 2/3 pyramidal cells. Intriguingly, neurotransmission from inhibitory fast-spiking interneurons appeared unaltered, despite being mediated by P/Q-type channels (i.e., carrying the FHM-1 mutation). This abnormal balance of cortical excitation-inhibition was associated with the increased susceptibility for CSD in the KI mice, but the underlying mechanism changing synaptic strength by the R192Q mutation is not fully understood. We used KI R192Q mice to study neurotransmission at the giant synapse known as the calyx of Held. This is a glutamatergic afferent forming on neurons of the Medial Nucleus of the Trapezoid Body (MNTB, Forsythe *et al*. 1994) where both presynaptic calcium currents (I_{pCa}) and excitatory postsynaptic currents (EPSCs) can be recorded. Since migraine is associated with cortical circuits (Aurora and Wilkinson, 2007), we extended our studies to cortical layer 2/3 pyramidal neurons, comparing Ca^{2+} currents elicited by different AP waveforms. We observed that KI presynaptic $Ca_V2.1$ channels activate at more hyperpolarized membrane potentials than WT channels. However, only a wide action potential can account for an increment in the evoked Ca^{2+} currents in KI mice compared to WT. Our observations may shed light on differential effects of FHM-1 mutations on different cortical synapses and thereby provide a better basis to understand the contribution of migraine mutations to pathology.

Materials and Methods

Generation of the R192Q KI mouse strain has been described previously (van den Maagdenberg *et al*. 2004). Both homozygous R192Q KI and WT mice from a similar genetic mixed background of 129 and C57BL6J were used for the experiments. All experiments were carried out according to National guidelines and approved by local Ethical Committees.

Preparation of brainstem and cortical slices.

Mice of P11-15 days were killed by decapitation, the brain removed rapidly and placed into an ice-cold low-sodium artificial cerebrospinal fluid (aCSF). The brainstem or cortical hemispheres containing motor cortex were mounted in the Peltier chamber of an Integraslice 7550PSDS microslicer (Campden Instruments Limited, UK). Transverse slices containing MNTB were cut sequentially and transferred to an incubation chamber containing low-calcium, normal-sodium aCSF at 37 ºC for 1h and returned at room temperature. Slices of either 200 or 300 μm thickness were used for presynaptic Ca^{2+} current recordings and for EPSC recordings, respectively. Normal aCSF contained (mM): NaCl 125, KCl 2.5, $NaHCO_3$ 26, NaH_2PO_4 1.25, glucose 10, ascorbic acid 0.5, myo inositol 3, sodium pyruvate 2, $MgCl_2$ 1 and $CaCl_2$ 2. Low sodium aCSF was as above but NaCl was replaced by 250 mM sucrose and $MgCl_2$ and $CaCl_2$ concentrations were 2.9 mM and 0.1 mM, respectively. The pH was 7.4 when gassed with 95% O_2-5% CO_2. Similarly, coronal slices including the motor cortex (180-250 μm) were obtained from P7–8 mice.

Electrophysiology

Slices were transferred to an experimental chamber perfused with normal aCSF at 25ºC. Neurons were visualized using Nomarski optics on a BX50WI microscope (Olympus, Japan) and a 60X/0.90 NA water immersion objective lens (LUMPlane FI, Olympus). Whole-cell voltage clamp recordings were made with patch pipettes pulled from thin walled borosilicate glass (Harvard Apparatus, GC150F-15, UK). Electrodes had resistances of 3.2-3.6 MΩ for presynaptic recordings and 3.0-3.4 MΩ for postsynaptic recordings, when filled with internal solution. Patch solutions for voltage clamp recordings contained (mM): CsCl 110, Hepes 40, TEA-Cl 10, Na_2phosphocreatine 12, EGTA 0.5, MgATP 2, LiGTP 0.5, QX-314 5 and $MgCl_2$ 1; pH was adjusted to 7.3 with CsOH. Lucifer Yellow was also included to visually confirm presynaptic recordings location.

Currents were recorded using a Multiclamp 700A amplifier (Axon Instruments, Union City, CA), a Digidata 1322A (Axon Instruments) and pClamp 9.0 software (Axon Instruments). Data were sampled at 50 kHz and filtered at 6 kHz (Low pass Bessel). Series resistance was compensated to be in the range 4-8 MΩ. Whole-cell membrane capacitances ranged 15-25 pF for calyx of Held terminals, and 28-36 pF for layer 2/3 pyramidal cells. Leak currents were subtracted on line with a P/5 protocol. Ca^{2+} currents were recorded in the presence of extracellular TTX (1 μM) and TEA-Cl (10 mM). EPSCs

were evoked by stimulating the globular bushy cell axons in the trapezoid body at the midline using a bipolar platinum electrode attached to an isolated stimulator (Stimuli of 0.1 ms, 4-10 V). Strychnine (1 µM) was added to the external solution to block inhibitory glycinergic synaptic responses.

Action potentials (APs) were measured in whole-cell configuration under current clamp mode. Patch solutions for current clamp recordings contained (mM): K^-Gluconate 110, KCl 30, Hepes 10, Na-phosphocreatine 10, EGTA 0.2, MgATP 2, LiGTP 0.5 and $MgCl_2$ 1. Only cells that had membrane resting potential between -60 mV to -75 mV were selected for recording. APs were elicited by injecting depolarizing step current pulses of 1-2 nA during 0.25 ms.

Average data are expressed and plotted as mean ± standard error of the mean (SEM). Statistical significance was determined using either Student's *t*-test or One-way ANOVA repeated measures plus Student-Newman-Keuls post-hoc test.

Results

Presynaptic calcium currents (I_{pCa}) and EPSCs from FHM-1 R192Q mice at the calyx of Held

We initially investigated the effect of the FHM1 R192Q mutation on the biophysical properties of presynaptic Ca^{2+} currents, which at the calyx of Held are almost exclusively mediated by P/Q-type Ca^{2+} channels. We examined the current-voltage (I-V) relationship of the presynaptic Ca^{2+} currents (I_{pCa}) at calyx of Held terminals following voltage-step depolarizations. Representative recordings are shown in figure 1A. In WT mice (n = 17), I_{pCa} activated around -45 mV, with a peak at -15 mV and showed an apparent reversal potential of around 55-60 mV. I_{pCa} activates at more hyperpolarizing potentials in R192Q KI calyx (n = 26), peaking at -20 mV, with similar reversal potential. In figure 1B, mean I_{pCa} amplitudes were normalized to the membrane capacitance of each presynaptic terminal. Maximum current amplitudes (measured at the potential corresponding to the peak of the I-V relationship) were not significantly different: 1150 ± 100 pA (current density 61 ± 3 pA/pF, n = 26) and 1050 ± 150 pA (current density 54 ± 3 pA/pF, n = 17) for KI and WT, respectively (Student´s *t*-test, $P > 0.05$). Activation curves obtained from the peak amplitudes of tail currents showed a -6.5 mV shift towards hyperpolarized potentials in KI compared to WT mice (figure 1C). Therefore, both IV and activation curves from R192Q KI presynaptic terminals are significantly different compared to WT (One-way ANOVA RM, Student-Newman-Keuls post-hoc, $P < 0.001$). Steady-state inactivation was measured using 2.5 s conditioning step potentials applied to presynaptic terminals, followed by a 50 ms test step to the potential at the peak of the I-V curve. Representative recordings are shown in figure 1D. Currents evoked by test voltage steps were normalized, plotted against voltage and fitted by the Boltzmann's function (figure 1E). Half-inactivation voltages $V_{1/2}$ were significantly more negative for R192Q KI compared to WT (Student´s *t*-test, $P = 0.017$).

In conclusion, R192Q KI mutation does affect biophysical properties of presynaptic Ca^{2+} currents: I_{pCa} are opened at more hyperpolarizing membrane potentials.

I_{pCa} elicited by AP waveforms from Calyx of Held terminals

Assuming that the kinetics of I_{pCa} can be modeled by Hodgkin/Huxley equations, a shift to more negative activation voltages should generate a larger Ca^{2+} current during an action potential (AP) (Borst and Sakmann, 1999). I_{pCa} were evoked by real AP waveforms previously recorded from the same preparation (see Materials and Methods). No differences in AP waveforms were observed between WT and R192Q KI synapses (figure 2A, upper traces). Since the duration of calyx of Held APs is shorter than 1 ms, it was important to have a good clamp of the membrane potential that assured effective voltage control during APs depolarization and repolarization. Membrane capacity and series resistance were well compensated and I_{pCa} recordings were accepted for analysis only if the presynaptic terminals were patch clamped under the following conditions: uncompensated series resistance below 12 MΩ and leak currents below 80 pA. Under these conditions, I_{pCa} had kinetics that were in agreement with those previously described (Fedchyshyn and Wang 2005, Takahashi 2005, Yang and Wang 2006). Mean traces of I_{pCa} evoked by the calyx of Held APs for both R192Q KI (n = 48) and WT mice (n = 30) are shown in figure 2A, bottom traces. There were no significant differences in mean I_{pCa} amplitudes between KI and WT calyx of Held presynaptic terminals (figure 2B, $P = 0.16$, Student's *t*-test). Mean half widths, decay times and rise times were also similar between WT and R192Q KI mice (figure 2C; $P>0.05$, Student's *t*-test). We concluded that the negative shift in activation of presynaptic Ca^{2+} channels in R192Q KI mice had little impact on Ca^{2+} currents when APs from calyx of Held were used as waveforms.

Evoked excitatory postsynaptic currents (EPSCs)

We analyzed transmitter release triggered by R192Q-mutated $Ca_v2.1$ channels. EPSCs evoked in both WT and R192Q KI mice showed synchronous release, displaying an all or nothing behaviour and having amplitudes (above threshold) that were independent of the stimulus intensity. EPSCs were abolished by ω-agatoxin IVA (200 nM), indicating that only P/Q-type channels are mediating Ca^{2+} influx responsible for transmitter release (data not shown). Figure 2D shows EPSCs recorded from the soma of an MNTB neuron under voltage clamp conditions at a holding potential of -70 mV. Mean EPSC amplitudes were identical: 10.6 ± 0.6 nA (n = 46) for WT and 10.7 ± 0.5 nA (n = 65) for KI (Student's *t*-test, $P = 0.42$).

Activity-dependent facilitation of presynaptic Ca^{2+} currents and transmitter release

Presynaptic calcium currents at the calyx of Held display Ca^{2+}-dependent facilitation which accounts for part of the facilitation of transmitter release, particularly under low depletion conditions (i.e., low Ca^{2+}- high Mg^{2+}; Felmy *et al.* 2003, Inchauspe *et al*. 2004; Muller *et al*. 2008). Pairs of AP waveforms with short inter-pulse intervals (5-10 ms) were applied under voltage-clamp to the

presynaptic terminals. With 2 mM [Ca^{2+}] in the external solution, the second I_{pCa} showed 12 ± 2% facilitation in R192Q KI (n = 12) and 10 ± 1% in WT mice (n = 10) (figure 2E). In 0.6 mM [Ca^{2+}] and 2 mM [Mg^{2+}], no difference was observed in EPSC paired-pulse facilitation: 44 ± 2% (n = 7) at R192Q KI and 45 ± 3% (n = 5) in WT calyx of Held synapses (figure 2F).

Ca^{2+} currents (I_{Ca}) in cortical layer 2/3 pyramidal cells

Since migraine has been suggested to be closely related to altered properties in cortical circuits (Aurora and Wilkinson, 2007), P/Q-type Ca^{2+} currents (I_{ca}) were recorded from layer 2/3 motor cortex PCs in brain slices from P10-11 WT and R192Q KI mice. To isolate P/Q type Ca^{2+} channels, N- and L-type blockers (ω–CgTxGVIA 1 μM and nitrendipine 10 μM, respectively) were added to the aCSF solution. Current-voltage curves (Figure 3A) showed a 6 mV hyperpolarizing shift in R192Q KI neurons, similar to data presented above from the calyx of Held and that published by Tottene *et al*. (2009) in pyramidal cells. P/Q-type Ca^{2+} currents were also evoked by AP waveforms previously recorded under current clamp from the same layer 2/3 PCs under the same experimental conditions mentioned above. Longer duration and lower amplitude APs were observed in pyramidal cells compared to the calyx of Held (Figure 3B, upper traces). The R192Q mutation significantly increased AP-evoked Ca^{2+} currents (Figure 3B lower traces and 3D left bars). In contrast, when P/Q-type I_{Ca} in layer 2/3 PCs were evoked by AP templates recorded at the calyx of Held, no difference in amplitude was observed between WT and R192Q KI mice (Figure 3C lower traces and 3D right bars). I_{Ca} kinetic parameters present no significant differences between WT and KI (figure 3E for PC AP-evoked I_{Ca} and figure 3F for calyx of Held AP-evoked I_{Ca}).

To systematically analyze the influence of AP time courses on I_{Ca}, we applied *pseudo-APs* with increasing repolarization times (from 0.1 to 1.9 ms) without changing the amplitude and depolarization time (0.5 ms) as shown in figure 4A. The I_{Ca} integral was plotted against repolarization time (figure 4B). The slope of the linear regression was larger for R192Q KI PCs compared to WT, confirming that I_{Ca} influx in R192Q KI PCs is larger when the waveform repolarization is prolonged.

Ca^{2+} currents (I_{Ca}) in cortical layer 2/3 pyramidal cells at physiological temperature

Temperature is well known to affect APs kinetics and voltage gated Ca^{2+} channels. We tested if the alterations described above at room temperature were reproduced at physiological temperature by recording APs from cortical layer 2/3 PCs at a temperature of 36±1ºC (figure 5A, top trace) and used these AP waveforms to generate I_{Ca} in PCs from both WT and R192Q KI mice (figure 5A, bottom traces). I_{Ca} recorded from R192Q KI PCs had bigger amplitudes compared to those recorded from WT (P = 0.001 Student's *t*-test, figure 5B). There were no significant differences in the kinetics of the Ca^{2+} currents between WT and R192Q KI mice (figure 5C). We then evoked I_{Ca} using ramp-shaped

waveforms with a rise time of 0.5 ms and different repolarization times to study the dependence of I_{Ca}-mediated charge with the duration of the APs at a temperature of 36±1ºC (figure 5D). We found a linear dependence of the calcium influx (i.e., time integral of the I_{Ca}) with repolarization time. The slope of the linear regression was significantly bigger in KI mice compared to WT mice (P = 0.008 Student's *t*-test, figure 6E). These results confirm that at physiological temperature the FHM1 mutation also induce an increase in Ca^{2+} currents when these are evoked by cortical PC-like APs.

I_{pCa} elicited by longer duration APs waveforms: calyx of Held vs cortical pyramidal cell APs

Tottene *et al*. (2009) have found a gain of function of excitatory neurotransmission at pyramidal cells from R192Q KI synapses. They propose that the increased probability of glutamate release at cortical layer 2/3 pyramidal cells results from an increased AP-evoked Ca^{2+} influx. Our results at the calyx of Held synapse indicated that the activation of the Ca^{2+} at more negative potentials did not imply an increment in AP-evoked Ca^{2+} currents. So we decided to study I_{pCa} at the presynaptic terminals from WT and R192Q KI mice with APs previously recorded from layer 2/3 pyramidal cells, which have longer duration and lower amplitude compared to the calyx of Held (Figure 6A, upper traces). When evoked by these PC APs, I_{pCa} from R192Q KI presynaptic calyceal terminals were significantly bigger compared to WT (figure 6A lower traces and 6B). However, kinetic parameters of the I_{pCa} at the calyx of Held evoked by the PC APs were not different between WT and KI (figure 6C).

In conclusion, our results suggest that activation of Ca^{2+} channels at more hyperpolarizing potentials led to higher inward Ca^{2+} influx during long duration/small amplitude APs (i.e., PC-like APs). However, negligible differences were observed when Ca^{2+} currents were elicited by short duration/large amplitude APs (i.e., calyx of Held-like APs). This may explain the unaltered inhibitory neurotransmission observed by Tottene *et al*. (2009) at the fast spiking interneuron- pyramidal cell synapses. Cortical layer 5/6 fast spiking interneurons (that have inhibitory projections into the pair connected PCs, generating brief IPSPs) have APs that are comparable in duration to those at the calyx of Held. Supplementary figure 1A shows representative repetitive AP firing from cortical layer 5/6 fast-spiking (FS) interneurons. In Supplementary figure 1B we superimposed APs from the calyx of Held, the cortical layer 2/3 PCs and from the cortical layer 5/6 fast spiking interneurons recorded from WT mice. The duration of APs from interneurons is known to be reduced at physiological temperature as well as in older animal (Ali et al. 2007).

Discussion

Using knock-in mice carrying the pathogenic FHM1 mutation R192Q in the α_{1A} subunit of P/Q-type Ca^{2+} channels, we evaluated the functional consequences of this mutation for Ca^{2+} currents from different neuronal types. At the calyx of Held synapse, the FHM1 mutation generates a hyperpolarizing shift of both activation and inactivation of $Ca_v2.1$ currents compared to WT. These alterations had little effect during AP-evoked presynaptic Ca^{2+} current recordings. This is an important result because it provides direct evidence that the FHM-1 mutations seen in the activation/inactivation parameters are not sufficient to elicit and alter the physiological phenotype at the calyx of Held. Presynaptic Ca^{2+} currents are generated during AP repolarization (i.e., when testing a more depolarizing voltage range compared to the range where differences in activation and inactivation properties had been investigated) and there are no differences in the I-V curves at potentials greater than 0 mV (Figure 1), so the absence of any gain of function in Ca^{2+} influx is not surprising.

At the calyx of Held in P11 and older mice, transmitter release is triggered exclusively by P/Q-type Ca^{2+} channels. Since no differences were observed in the AP-evoked I_{pCa} we expected no differences in neurotransmitter output. Accordingly, the FHM-1 mutated $Ca_V2.1$ Ca^{2+} channels in R192Q KI mice mediate functional transmission with similar EPSC amplitudes, release probability and facilitation than WT mice. These results contrast with the increased release probability of the glutamatergic pyramidal cell synapses recently reported by Tottene *et al*. (2009). Nevertheless, they agree with the normal transmitter release observed at the fast spiking interneuron inhibitory synapses and at the neuromuscular junction studied in the same animal model (Kaja *et al* .2005, Tottene *et al.* 2009).

Tottene *et al*. (2009) suggested that the increased probability of glutamate release at cortical layer 2/3 pyramidal cells results from an increased AP-evoked Ca^{2+} influx (related to the shift in the activation potential of the mutated Ca^{2+} channels), but experimental proof was not provided. To test the hypothesis that increased AP-evoked Ca^{2+} currents in the cortical pyramidal neurons was due to changes in Ca^{2+} channel activation, the depolarization and hyperpolarization rates of the AP waveforms must be taken into account (Bischofberger *et al.* 2002, Li *et al.* 2007). We used APs recorded from the cortical layer 2/3 PCs and from the calyx of Held to compare the I_{Ca} elicited by both AP waveforms. While I_{Ca} amplitudes recorded in WT or KI cortical layer 2/3 pyramidal cells showed no differences when elicited by calyx of Held AP waveforms, a significant increase in the amplitude of I_{Ca} was observed in R192Q KI compared to WT when pyramidal cell AP waveforms were used. Likewise, KI mice do show an enhancement in I_{pCa} at the calyx of Held presynaptic terminals when elicited by PC APs. Thus, our results strongly suggest that synapses driven by larger amplitude and shorter duration APs (e.g., Calyx of Held and interneurons APs) are affected less by the mutation-induced

hyperpolarizing shift in voltage-dependence of Ca^{2+} channel activation, than those driven by longer duration APs (e.g., pyramidal neurons APs). Moreover, we have shown that I_{Ca} influx elicited using AP-like waveforms with different repolarization times became significantly larger in KI pyramidal neurons compared to WT when the waveform repolarization phase was prolonged. The driving force for Ca^{2+} ions develops during repolarization of the AP, reaching the highest values closer to the resting potential where the shift in the I-V curve found in the FHM-1 mutated channel is more significant. A decrease in the rate of repolarization will increase the contribution of the Ca^{2+} currents at hyperpolarizing potential values, allowing the difference in activation due to the channel mutation to be expressed and so leading to an increase in total Ca^{2+} current. We have confirmed that our conclusions are also valid at physiological temperature (where APs and I_{ca} have faster kinetics compared to room temperature). We also found that after calcium channels were opened for a long period of time, their voltage dependence of inactivation was shifted towards more negative potential values (a -5 mV shift in half-inactivation voltages). Since this shift in voltage-dependence steady state inactivation of the mutated calcium channels depends on previous activation of the channels during seconds, we believe that it would not introduce significant differences during simple AP-evoked Ca^{2+} currents. However, during repetitive firing at high frequencies, the inactivation at more hyperpolarizing potentials may prevent small conductance calcium-activated potassium channels (SK) from being activated during the train of APs. Therefore, a twofold increment in excitability at cortical networks might be taking place: 1) due to increasing Ca^{2+} currents in KI during PC APs (voltage shift of activation) and 2) because of decreasing activation of SK currents during repetitive APs discharge. These alterations would facilitate induction and propagation of cortical spreading depression (CSD) in KI mice.

The differences in AP durations that trigger cortical excitatory and inhibitory synapses may explain the unaltered inhibitory neurotransmission observed at the fast spiking (FS) interneuron-pyramidal cell (PC) synapses and the gain of function observed at the PC-FS interneuron excitatory synapses. Ali et al. (2007) measured the APs of several types of interneurons (in juvenile/adult cats and rats) and found that multipolar interneurons that display fast spiking behavior with little or no spike accommodation have APs with half-widths between 0.2-0.3 ms in adult species and between 0.8-1.3 ms in juveniles, whereas interneurons with burst or adapting firing patterns (e.g., bitufted interneurons) exhibited APs with a wide range of half-widths (0.2-0.6 ms in adults and 1.2-1.8 ms in juveniles). The presynaptic basket cells are another example of neurons displaying fast spiking APs of very short duration., Bucurenciu *et al*. (2010) precisely describe that a small number of Ca^{2+} channels are necessary to trigger and evoke transmitter release with high temporal precision at the gabaergic basket cell - granule cells synapse in the dentate gyrus of rat hippocampal slices, supporting the hypothesis that at inhibitory synapses controlled by short APs the activation of the FHM1 mutated channels at more negative potentials have little or no effect in transmitter release. The ideal test of our hypothesis would be to

measure the presynaptic AP waveform in cortical nerve terminals but this is not possible. However a good correlation between the half-width of the somatic action potential and the synaptic events elicited in and by interneurons has been reported (Ali *et al*. 2007), indicating that at the presynaptic nerve terminal variations in AP duration are rather small compared to the difference in duration and amplitude observed between the calyx of Held or the fast spiking interneurons and the cortical APs. Simultaneous recording of axon and somatic APs in neocortical PCs have a similar time course, although the amplitudes of the former are reduced (Shu *et al.* 2007) favoring the expression of altered gating properties of the mutated Ca^{2+} channels.

Several mechanisms may contribute to the differential effect of FHM-1 mutations at different synapses, including different isoforms of the mutated α1 subunit or differences in the G-protein modulation of Ca^{2+} channels (Weiss *et al.* 2008), but our data provide evidence that the AP time-course is a crucial element in regulating Ca^{2+} influx into nerve terminals and determining synaptic gain of function.

Acknowledgements

This work was supported by Wellcome Trust grant RM36 046**,** UK and UBACYT X-171, Universidad de Buenos Aires, Argentina (to Dr. Uchitel), FONCYT-ANPCyT BID 1728 OC.AR. PICT 2007-1009, PICT 2008-2019 and PIDRI-PRH 2007 (to Dr. Urbano) and the Centre for Medical Systems Biology (CMSB) in the framework of the Netherlands Genomics Initiative (NGI) (to Dr. van den Maagdenberg).

We would like to thank María Eugenia Martin and Paula Felman for their invaluable technical and administrative assistance.

References

Ali AB, Bannister AP and Thomson AM. Robust correlations between action potential duration and the properties of synaptic connections in layer 4 interneurones in neocortical slices from juvenile rats and adult rat and cat. J. Physiol. 580: 149-169, 2007.

Aurora SK and Wilkinson F. The brain is hyperexcitable in migraine. Cephalalgia 27:1442-1453, 2007.

Barrett CF, Cao YQ and Tsien RW. Gating deficiency in a familial hemiplegic migraine type 1 mutant P/Q-type calcium channel. J. Biol. Chem. 280: 24064-24071, 2005.

Bischofberger J, Geiger JR and Jonas P. Timing and efficacy of Ca^{2+} channel activation in hippocampal mossy fiber boutons. J Neurosci. 22: 10593-10602, 2002.

Borst JG and Sakmann B. Effect of changes in action potential shape on calcium currents and transmitter release in a calyx-type synapse of the rat auditory brainstem. Philos Trans R Soc Lond B Biol Sci 354: 347-355, 1999.

Bucurenciu I, Bischofberger J and Jonas P. A small number of open Ca^{2+} channels trigger transmitter release at a central GABAergic synapse. Nature Neuroscience 13: 19-21, 2010.

Cao YQ and Tsien RW. Effects of familial hemiplegic migraine type 1 mutations on neuronal P/Q-type Ca2+ channel activity and inhibitory synaptic transmission. Proc. Natl. Acad. Sci. U S A. 102: 2590-2595, 2005.

Fedchyshyn M J and Wang L. Developmental transformation of the release modality at the calyx of Held synapse. The Journal of Neuroscience 25: 4131-4140, 2005.

Felmy F, Neher E and Schneggenburger R. Probing the intracellular calcium sensitivity of transmitter release during synaptic facilitation. Neuron 37(5): 801-11, 2003.

Ferrari MD, van den Maagdenberg AMJM, Frants RR and Goadsby PJ (2008) Molecular Neurology. Migraine as a cerebral ionopathy with impaired central sensory processing. Waxman, S.G. (editor): 439-461.

Forsythe ID. Direct patch recording from identified presynaptic terminals mediating glutamatergic EPSCs in the rat CNS, in vitro. J Physiol. 479: 381-387, 1994.

González Inchauspe C, Forsythe ID and Uchitel OD. Changes in synaptic transmission properties due to the expression of N-type calcium channels at the calyx of Held synapse of mice lacking P/Q-type calcium channels. Journal of Physiology 584: 835-51, 2007.

Hans M, Luvisetto S, Williams ME, Spagnolo M, Urrutia A, Tottene A, Brust PF, Johnson EC, Harpold MM, Stauderman KA and Pietrobon D. Functional consequences of mutations in the human α_{1A} calcium channel subunit linked to familial hemiplegic migraine. J Neurosci. 19: 1610-1619, 1999.

Inchauspe C, Martini FJ, Forsythe ID and Uchitel OD. Functional compensation of P/Q by N-type channels blocks short-term plasticity at the calyx of Held presynaptic terminal. J Neurosci 24: 10379-10383, 2004.

Iwasaki S and Takahashi T. Developmental changes in calcium channel types mediating synaptic transmission in rat auditory brainstem. J. Physiol. 509: 419-423, 1998.

Iwasaki S, Momiyama A, Uchitel OD and Takahashi T. Developmental Changes in Calcium Channel Types Mediating Central Synaptic Transmission. J. Neurosci**.** 20: 59-65, 2000.

Kaja S, van de Ven RC, Broos LA, Veldman H, van Dijk JG, Verschuuren JJ, Frants RR, Ferrari MD, van den Maagdenberg AM and Plomp JJ. Gene dosage-dependent transmitter release changes at neuromuscular synapses of *CACNA1A* R192Q knockin mice are non-progressive and do not lead to morphological changes or muscle weakness. Neuroscience 135: 81-95, 2005.

Kraus RL, Sinnegger MJ, Glossmann H, Hering S and Striessnig J. Familial hemiplegic migraine mutations change α_{1A} Ca^{2+} channel kinetics. J. Biol. Chem. 273: 5586-5590, 1998.

Kraus RL, Sinnegger MJ, Koschak A, Glossmann H, Stenirri S, Carrera P and Striessnig J. Three new familial hemiplegic migraine mutants affect P/Q-type Ca(2+) channel kinetics. J. Biol. Chem. 275: 9239-9243, 2000.

Lauritzen M. Pathophysiology of the migraine aura: The spreading depression theory. Brain 117**:** 199-210, 1994.

Li L, Bischofberger J and Jonas P. Differential gating and recruitment of P/Q-,N-, and R-type Ca2+ channels in hippocampal mossy fiber boutons. J Neurosci. 27: 13420-13429, 2007.

Muller M, Felmy F and Schneggenburger R. A limited contribution of Ca^{2+} current facilitation to paired-pulse facilitation of transmitter release at the rat calyx of Held. J Physiol (Lond) 586: 5503-5520, 2008.

Shu Y, Duque A, Yu Y, Haider B and McCormick DA. Properties of Action-Potential Initiation in Neocortical Pyramidal Cells: Evidence From Whole Cell Axon Recordings. J Neurophysiol 97: 746-

760, 2007.

Takahashi T. Dynamic aspects of presynaptic calcium currents mediating synaptic transmisión. Cell Calcium 37: 507–511, 2005.

Tottene A, Fellin T, Pagnutti S, Luvisetto S, Striessnig J, Fletcher C and Pietrobon D. Familial hemiplegic migraine mutations increase Ca^{2+} influx through single human $Ca_V2.1$ channels and decrease maximal $Ca_V2.1$ current density in neurons. Proc. Natl. Acad. Sci. (PNAS) 99: 13284-13289, 2002.

Tottene A, Pivotto F, Fellin T, Cesetti T, van den Maagdenberg AMJM and Pietrobon D. Specific Kinetic Alterations of Human $Ca_V2.1$ Calcium Channels Produced by Mutation S218L Causing Familial Hemiplegic Migraine and Delayed Cerebral Edema and Coma after Minor Head Trauma. J. Biol. Chem. 280: 17678-17686, 2005.

Tottene A, Conti R, Fabbro A, Vecchia D, Shapovalova M, Santello M, van den Maagdenberg AM, Ferrari MD and Pietrobon D. Enhanced excitatory transmission at cortical synapses as the basis for facilitated spreading depression in Ca(v)2.1 knockin migraine mice. Neuron 61: 762-73, 2009.

van den Maagdenberg AM, Pietrobon D, Pizzorusso T, Kaja S, Broos LA, Cesetti T, van de Ven RC, Tottene A, van der Kaa J, Plomp JJ, Frants RR and Ferrari MD. A *Cacna1a* Knockin Migraine Mouse Model with Increased Susceptibility to Cortical Spreading Depression. Neuron 41: 701-710, 2004.

Weiss N, Sandoval A, Felix R, Van den Maagdenberg AM and De Waard M. The S218L familial hemiplegic migraine mutation promotes deinhibition of Cav2.1 calcium channels during direct G-protein regulation. Pflugers Arch. 457: 315-326, 2008.

Yang YM and Wang LY. Amplitude and kinetics of action potential-evoked Ca^{2+} current and its efficacy in triggering transmitter release at the developing calyx of Held synapse. The Journal of Neuroscience 23: 5698-5708, 2006.

Figure legends

Figure 1 - Properties of presynaptic Ca^{2+} currents at the calyx of Held from WT and R192Q KI mice

A- I_{pCa} (below) evoked by 20 ms depolarizing voltage steps (above) from -75 mV to potentials ranging -60 to 60 mV (5 mV steps). Right insets: tail currents elicited after repolarization to -75 mV.

B- I/V relationship for I_{pCa} from WT (n = 17) and R192Q KI (n = 26).

C- I_{pCa} activation curves: normalized amplitudes of tail currents plotted against voltage and fitted by the Boltzmann's function: $I(V) = 1/[(1 + \exp((V- V_{1/2})/k)]$. Half-activation voltages ($V_{1/2}$) were -32.4 ± 0.3 mV for R192Q KI (n = 26) and -25.9 ± 0.2 mV for WT (Student's *t*-test, $P = 6x10^{-6}$, n = 17) and slope factors (*k)*: 4.75 ± 0.25 mV and 6.0 ± 0.2 mV ($P = 0.035$, Student´s *t*-test) for R192Q KI and WT respectively.

D- I_{pCa} evoked by a 50 ms voltage step to the peak of the I-V curve, after applying conditioning prepulses for 2.5 s to different voltages from -75 to -15 mV (2.5 mV steps).

E- Steady state inactivation of I_{pCa} from R192Q KI and WT terminals. Data are normalized to the maximum peak amplitude, plotted against the conditioning voltage and fitted by the Boltzmann's function. Half-inactivation voltages $V_{1/2}$ were significantly more negative (-39.2 ± 0.2 mV, n = 12) for R192Q KI compared to WT (-35.5 ± 0.1 mV, n = 6; Student´s *t*-test, $P = 0.017$). Slopes were: -4.0 ± 0.2 mV and -4.8 ± 0.1 mV (Student´s *t*-test, $P = 0.06$) for R192Q KI and WT, respectively.

* Significant differences between WT and R192Q KI mice ($P < 0.001$, One-way ANOVA RM, Student-Newman-Keuls post-hoc).

Figure 2 - AP-evoked presynaptic calcium currents (I_{pCa}) and EPSCs at calyx of Held from WT and R192Q KI mice.

A- Upper traces: average APs waveforms at the calyx of Held from WT (dotted black, n = 4) and R192Q KI (grey, n = 3) mice. Mean potential amplitude was 110 ± 2 mV and 112 ± 2 mV, Half-width: 0.44 ± 0.02 ms and 0.44 ± 0.03 ms, rise time (10-90%): 0.33 ± 0.02 ms and 0.31 ± 0.04 ms and decay time 0.40 ± 0.02 ms and 0.44 ± 0.04 ms for WT and R192Q KI mice, respectively. Bottom traces: mean I_{pCa} elicited by APs (dotted black and grey traces for WT and R192Q KI, respectively).

B - Mean I_{pCa} amplitudes evoked by APs at the calyx of Held presynaptic terminals are not significantly different between WT and R192Q KI mice

C – Kinetic parameters of presynaptic Ca^{2+} currents at the calyx of Held synapses generated by their own APs (n = 30 for WT and n = 48 for R192Q KI mice).

D- Representative EPSCs evoked in MNTB neurons from WT (dotted black) and R192Q KI (grey) mice at a holding potential of -70 mV, in 2 mM $[Ca^{2+}]_o$ aCSF.

E- Presynaptic Ca^{2+} current facilitation. Pairs of AP waveforms evoked I_{pCa} showing activity-dependent facilitation in WT and R192Q KI. Mean pair pulse facilitation was 12 ± 2% in R192Q KI (n = 12) and 10 ± 1% in WT mice (n = 10).

F - Facilitation of EPSCs. A pair of stimuli was applied with a short interval (10 ms). In low external Ca^{2+} concentration (0.6 mM) and high external Mg^{2+} concentration (2 mM), the EPSC evoked by the second stimulus is facilitated with respect to the first EPSC in synapses from both WT (45 ± 3%, n = 5) and R192Q KI mice (44 ± 2%, n = 7).

Figure 3 - AP-evoked P/Q-type Ca^{2+} currents (I_{Ca}) in layer 2/3 pyramidal cells (PC) from WT and KI cortical slices.

A - P/Q-type current density as a function of voltage in WT and R192Q KI layer 2/3 pyramidal cells (PC). Normalized I-V curves were multiplied by the average maximal current density (6.9 ± 0.3 pA/pF, n = 7 for WT and 8.2 ± 0.2 pA/pF, n = 7 for KI).

* Significant differences between WT and R192Q KI mice ($P < 0.001$, One-way ANOVA RM, Student-Newman-Keuls post-hoc).

B- Upper traces: AP waveforms recorded in PCs (dotted black for WT and grey for R192Q KI mice, offset for better visualisation). WT PCs had APs with a mean rise time of 0.53 ± 0.05 ms; half-width of 1.97 ± 0.08 ms; decay time of 3.1 ± 0.2 ms and potential amplitude of 90 ± 2 mV (n = 5). Similar values were measured from KI mice (rise time: 0.52 ± 0.07 ms; half-width: 1.72 ± 0.12 ms; decay time: 2.9 ± 0.4 ms; potential amplitude: 92 ± 2 mV; n = 6). Bottom traces: I_{Ca} elicited by the above APs in the same cells (black for WT and grey for R192Q KI mice).

C- I_{Ca} in PC (bottom traces, dotted black for WT, grey for KI mice) evoked by the AP waveforms (upper traces) recorded at the calyx of Held presynaptic terminals.

D- Mean I_{Ca} amplitude evoked in PCs by either AP waveforms showed in B and C. I_{Ca} amplitudes from KI PCs (240 ± 15 pA, n = 25) are 41 % larger than those from WT PCs (170 ± 10 pA, n = 18, $P = 0.01$) when evoked by PC APs. I_{Ca} were not statistically different when evoked by calyx of Held APs. Mean amplitudes were: 402 ± 27 pA for R192Q KI mice (n =25) and 345 ± 26 pA for WT mice (n = 18; Student's *t*-test, $P = 0.07$).

E- Kinetic parameters of Ca^{2+} currents generated in PCs by AP waveforms corresponding to the same cells (n = 18 for WT and n = 25 for R192Q KI mice).

F- Kinetic parameters of Ca^{2+} currents generated in PCs by AP waveforms of the calyx of Held (n =18 for WT and n = 25 for R192Q KI mice).

Figure 4 - Dependence of calcium influx with the AP repolarization rate

A- Recordings of I_{Ca} in response to AP-like voltage ramps (from -65 mV to +20 mV, rise time of 0.5 ms, plateau duration of 0.05 ms and increasing decay times from 0.1 to 1.9 ms with 0.2 ms increments) in WT and R192Q KI pyramidal cells.

B- I_{Ca}-mediated charge (I_{Ca} integral) is plotted as a function of the AP repolarization time. Solid lines show the linear regression of the data. Slope value is larger for R192Q KI mice (136±3 pA, n = 12) than for WT mice (99±3 pA, n = 13, Student's *t*-test, $P = 0.002$).

* Significant differences between WT and R192Q KI mice ($P < 0.006$, One-way ANOVA RM, Student-Newman-Keuls post-hoc).

Figure 5 - AP-evoked P/Q-type Ca^{2+} currents (I_{Ca}) in layer 2/3 pyramidal cells (PC) from WT and KI cortical slices at physiological temperature.

A- Upper traces: AP waveforms recorded in PCs at physiological temperature (36 ± 1ºC). Mean rise time was 0.41 ± 0.03 ms; half-width 0.93 ± 0.04 ms; decay time 1.9 ± 0.3 ms and potential amplitude 85 ± 3 mV (n = 6). Bottom traces: I_{Ca} elicited by the above APs in PC at physiologival temperature (black for WT and grey for R192Q KI mice).

B- Mean I_{Ca} amplitude evoked in PCs by their own APs at physiological temperature are 35 % larger in R192Q KI mice (380 ± 22, n = 27, $P = 0.001$ Student's *t*-test) than in WT mice (280 ± 22 pA, n = 32).

C- Kinetic parameters of Ca^{2+} currents generated in PCs by AP waveforms corresponding to the same cells (n = 32 for WT and n = 27 for R192Q KI) at 36 ± 1ºC.

D- Recordings of I_{Ca} in response to AP-like voltage ramps (from -65 mV to +20 mV, rise time of 0.5 ms, plateau duration of 0.05 ms and increasing decay times from 0.1 to 2.1 ms with 0.2 ms increments) in WT and R192Q KI pyramidal cells at 36 ± 1ºC.

E - I_{Ca}-mediated charge (I_{Ca} integral) is plotted as a function of the AP repolarization time. Solid lines show the linear regression of the data. Slope value is larger for R192Q KI mice (230±3 pA, n = 18) than for WT mice (177±2 pA, n = 18, Student's *t*-test, $P = 0.008$).

* Significant differences between WT and R192Q KI mice ($P < 0.005$, One-way ANOVA RM, Student-Newman-Keuls post-hoc).

Figure 6 - I_{pCa} at the calyx of Held evoked by long AP waveforms recorded at pyramidal cells (PCs).

A - Upper traces: AP waveforms recorded in PCs (dotted black for WT and grey for R192Q KI mice, offset for better visualisation, see parameters in figure legend 3B). Bottom traces: I_{pCa} elicited by the above APs at the calyx of Held presynaptic terminals (dotted black for WT and grey for R192Q KI mice).

B - Mean I_{pCa} amplitudes evoked at the calyx of Held presynaptic terminals by the PCs APs are 41 %

570 larger at KI mice (650 ± 58 pA, n = 24) than at WT mice (460 ± 44 pA, n = 11, *P* = 0.018, Student's *t*-
571 test).
572 C- Kinetic parameters of presynaptic Ca^{2+} currents at the calyx of Held synapses generated by AP
573 waveforms from pyramidal cells (n = 11 for WT and n = 24 for R192Q KI mice).
574
575 **Supplementary figure 1- Inhibitory synapses usually have short duration presynaptic APs**
576 A- Firing pattern of a layer 5/6 fast-spiking (FS) interneuron in cortical slices from WT mice, obtained
577 in current clamp mode by small supra-threshold depolarizing current injections (50-200 pA, 100 ms).
578 APs have a mean rise time of 0.50 ± 0.03 ms; half-width of 1.12 ± 0.04 ms; decay time of 1.2 ± 0.3 ms
579 and potential amplitudes of 102 ± 1 mV (n = 8).
580 B- Superimposed mean APs from the calyces of Held, the cortical layer 2/3 PCs and the cortical layer
581 5/6 fast spiking interneurons of WT mice at room temperature.
582 APs were recorded at a sampling frequency 50 kHz using a Multiclamp 700A amplifier (Axon
583 Instruments, Union City, CA), a Digidata 1322A (Axon Instruments) and pClamp 9.0 software (Axon
584 Instruments). Patch solutions for current clamp recordings contained (mM): K^-Gluconate 110, KCl 30,
585 Hepes 10, Na-phosphocreatine 10, EGTA 0.2, MgATP 2, LiGTP 0.5 and $MgCl_2$ 1.
586
587

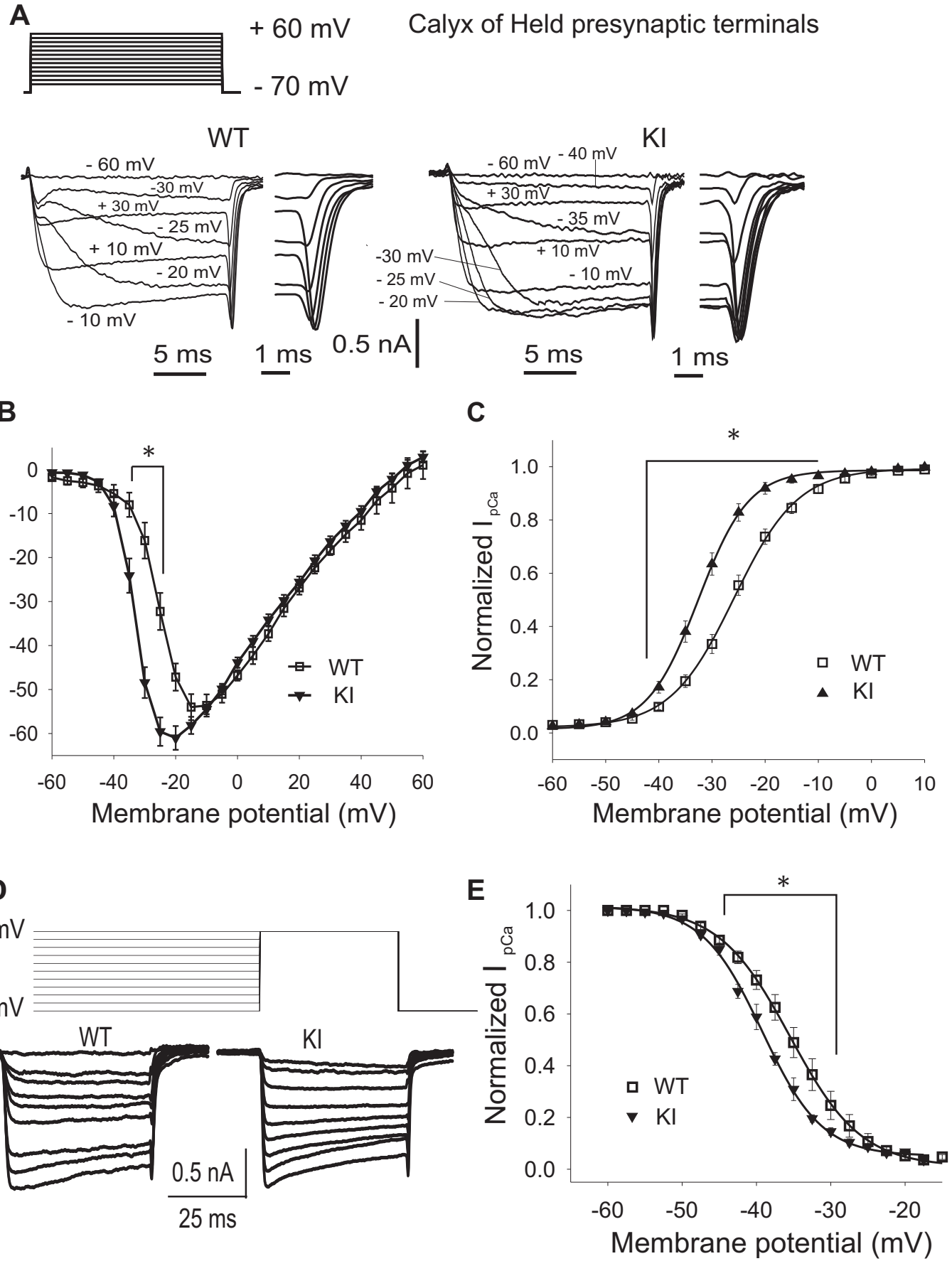
A
+ 60 mV
- 70 mV
Calyx of Held presynaptic terminals
WT
KI
- 60 mV
-30 mV
+ 30 mV
- 25 mV
+ 10 mV
- 20 mV
- 10 mV
- 40 mV
- 35 mV
5 ms
1 ms
0.5 nA
B
C
*
I_{pCa} density (pA/pF)
Membrane potential (mV)
Normalized I_{pCa}
WT
KI
D
- 15mV
- 75 mV
25 ms
E

Figure 1

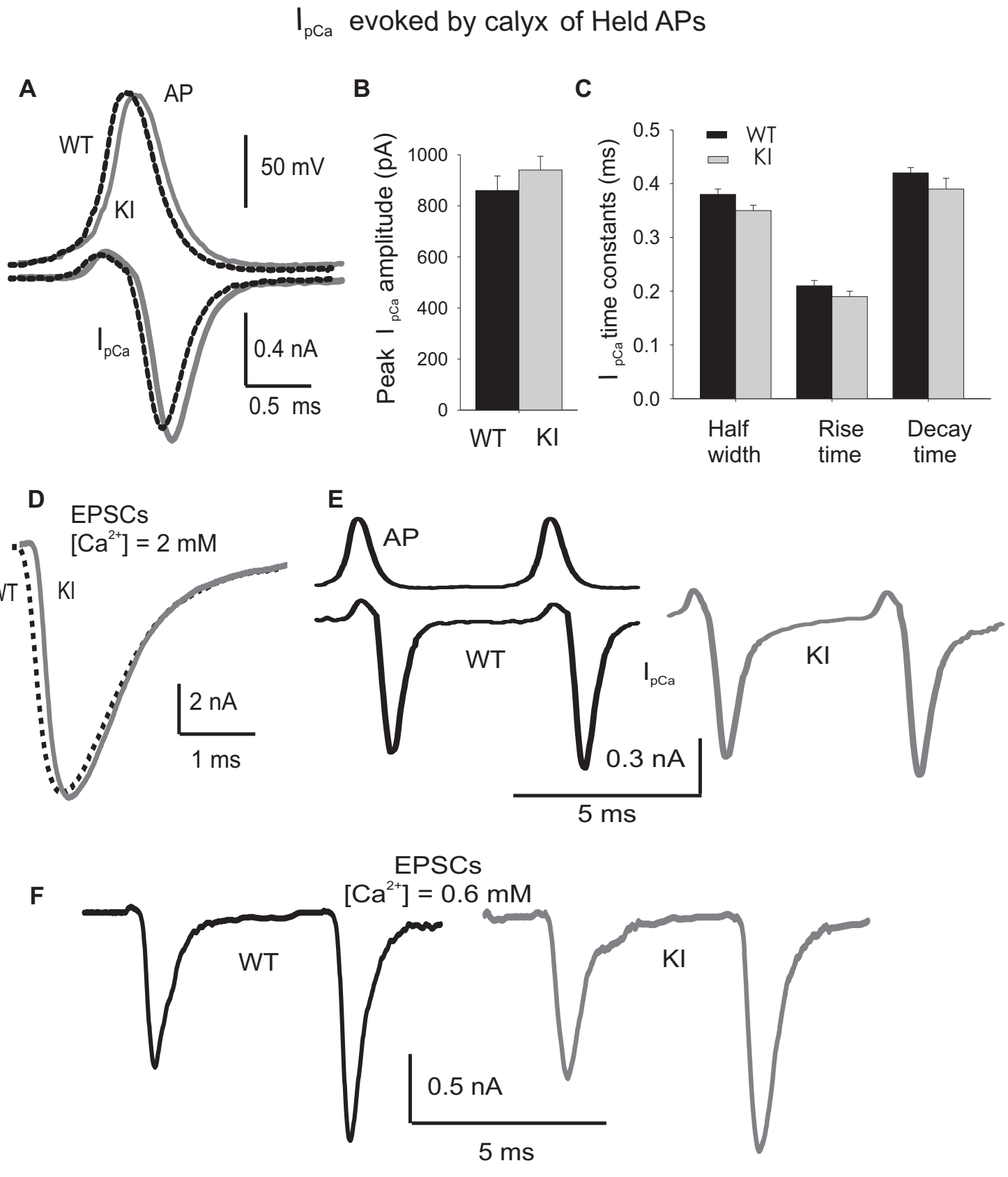
I_{pCa} evoked by calyx of Held APs
A
AP
WT
KI
50 mV
I_{pCa}
0.4 nA
0.5 ms
B
Peak I_{pCa} amplitude (pA)
1000
800
600
400
200
0
WT
KI
C
I_{pCa} time constants (ms)
0.5
0.4
0.3
0.2
0.1
0.0
WT
KI
Half width
Rise time
Decay time
D
EPSCs
$[Ca^{2+}]$ = 2 mM
WT
KI
2 nA
1 ms
E
AP
WT
I_{pCa}
KI
0.3 nA
5 ms
F
EPSCs
$[Ca^{2+}]$ = 0.6 mM
WT
KI
0.5 nA
5 ms

Figure 2

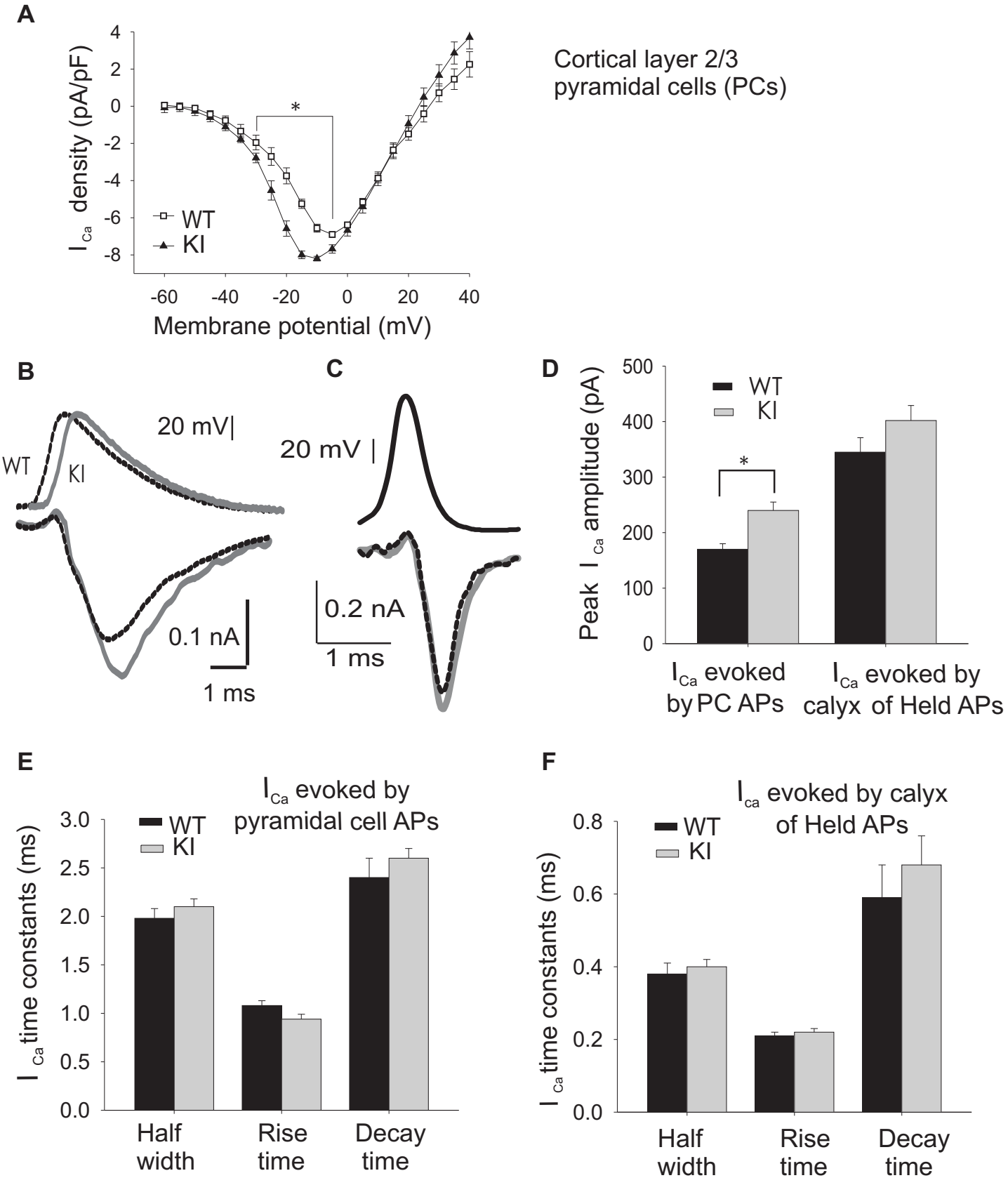
A
Cortical layer 2/3
pyramidal cells (PCs)
I Ca density (pA/pF)
WT
KI
Membrane potential (mV)
B
20 mV
WT
KI
0.1 nA
1 ms
C
20 mV
0.2 nA
1 ms
D
Peak I Ca amplitude (pA)
WT
KI
I Ca evoked by PC APs
I Ca evoked by calyx of Held APs
E
I Ca evoked by pyramidal cell APs
WT
KI
I Ca time constants (ms)
Half width
Rise time
Decay time
F
I ca evoked by calyx of Held APs
WT
KI
I Ca time constants (ms)
Half width
Rise time
Decay time

Figure 3

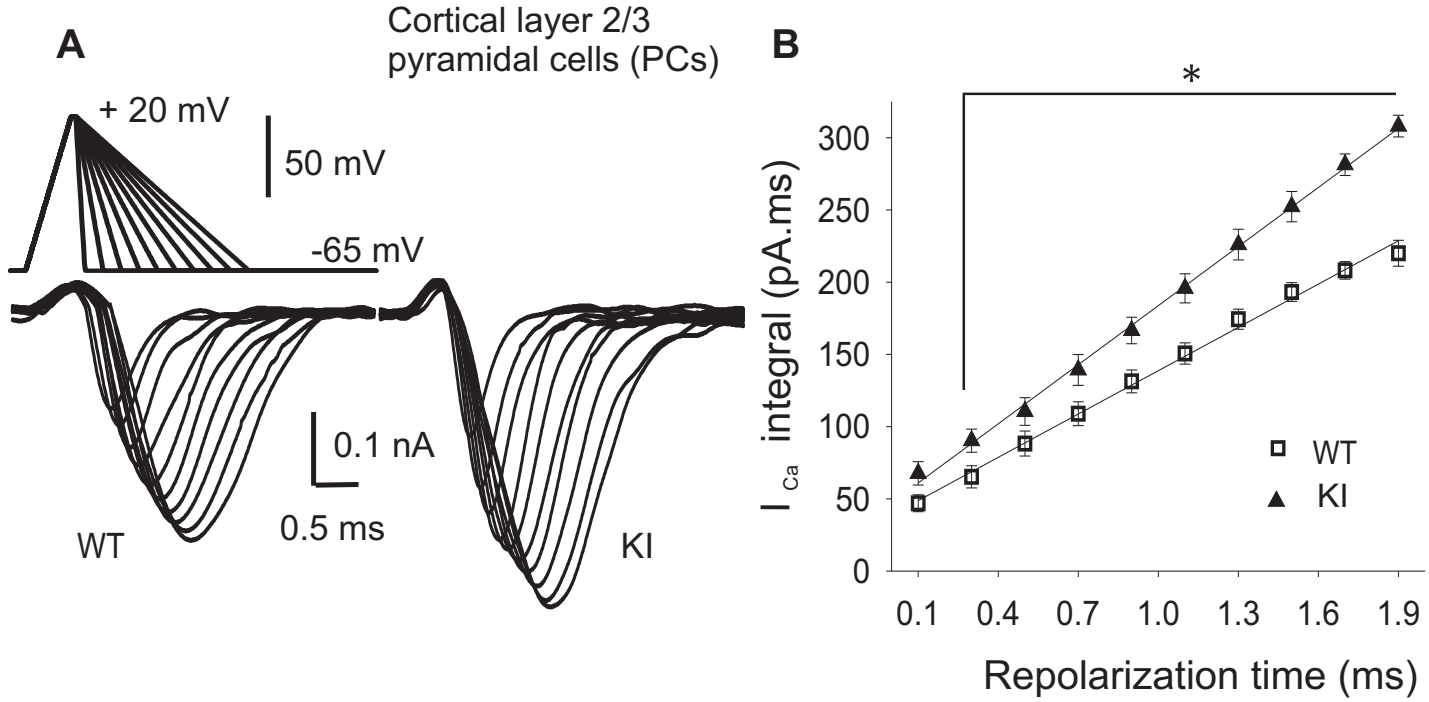
A
Cortical layer 2/3
pyramidal cells (PCs)
+ 20 mV
50 mV
-65 mV
0.1 nA
0.5 ms
WT
KI
B
*
I_{Ca} integral (pA.ms)
300
250
200
150
100
50
0
0.1
0.4
0.7
1.0
1.3
1.6
1.9
WT
KI
Repolarization time (ms)

Figure 4

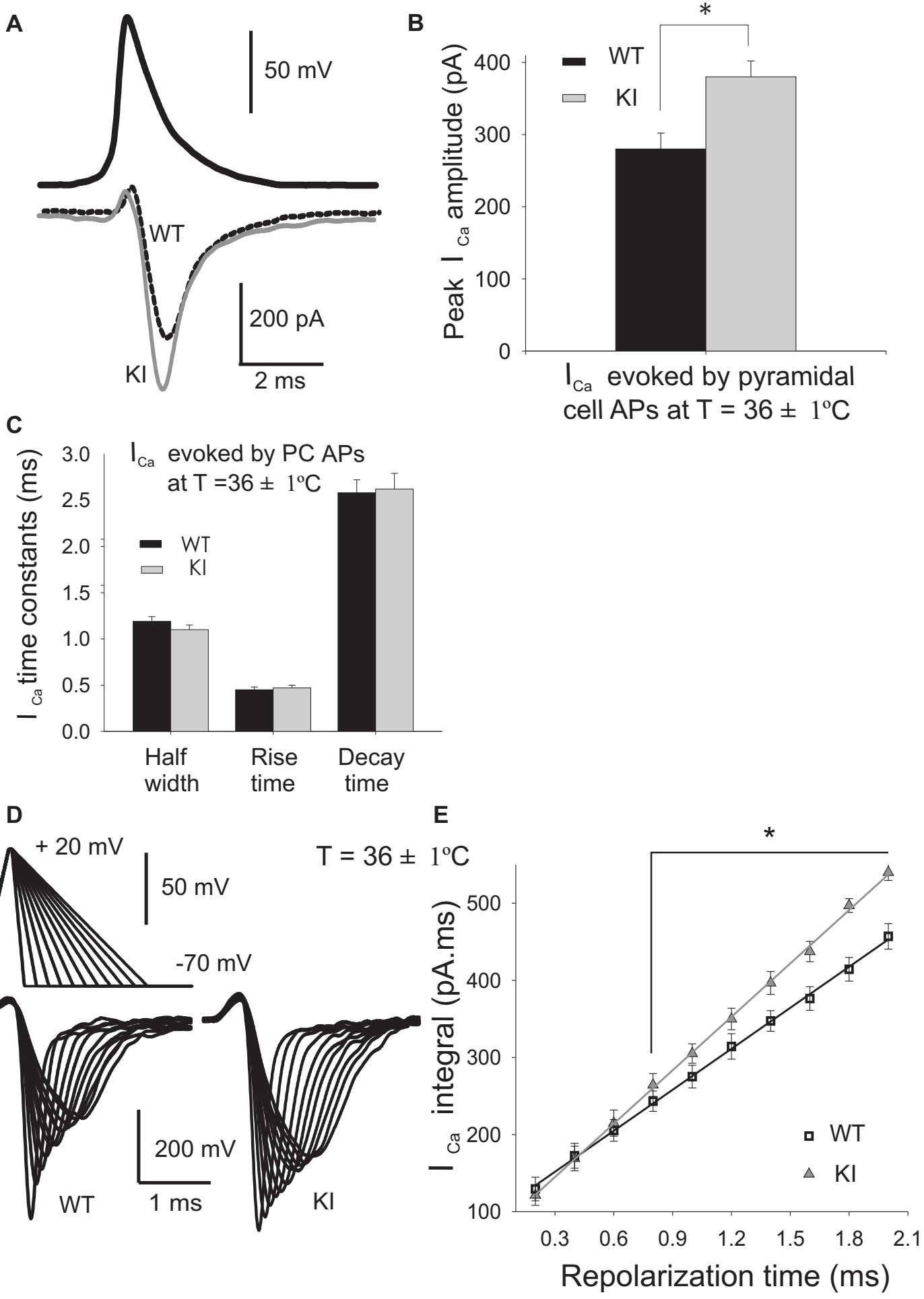
A
50 mV
WT
200 pA
KI
2 ms
B
*
WT
KI
Peak I_{Ca} amplitude (pA)
400
300
200
100
0
I_{Ca} evoked by pyramidal cell APs at T = 36 ± 1ºC
C
I_{Ca} evoked by PC APs at T =36 ± 1ºC
WT
KI
I_{Ca} time constants (ms)
3.0
2.5
2.0
1.5
1.0
0.5
0.0
Half width
Rise time
Decay time
D
+ 20 mV
50 mV
-70 mV
T = 36 ± 1ºC
200 mV
1 ms
WT
KI
E
*
I_{Ca} integral (pA.ms)
500
400
300
200
100
WT
KI
0.3
0.6
0.9
1.2
1.5
1.8
2.1
Repolarization time (ms)

Figure 5

Presynaptic Ca^{2+} currents (I_{pCa}) at the Calyx of Held evoked by pyramidal cell APs

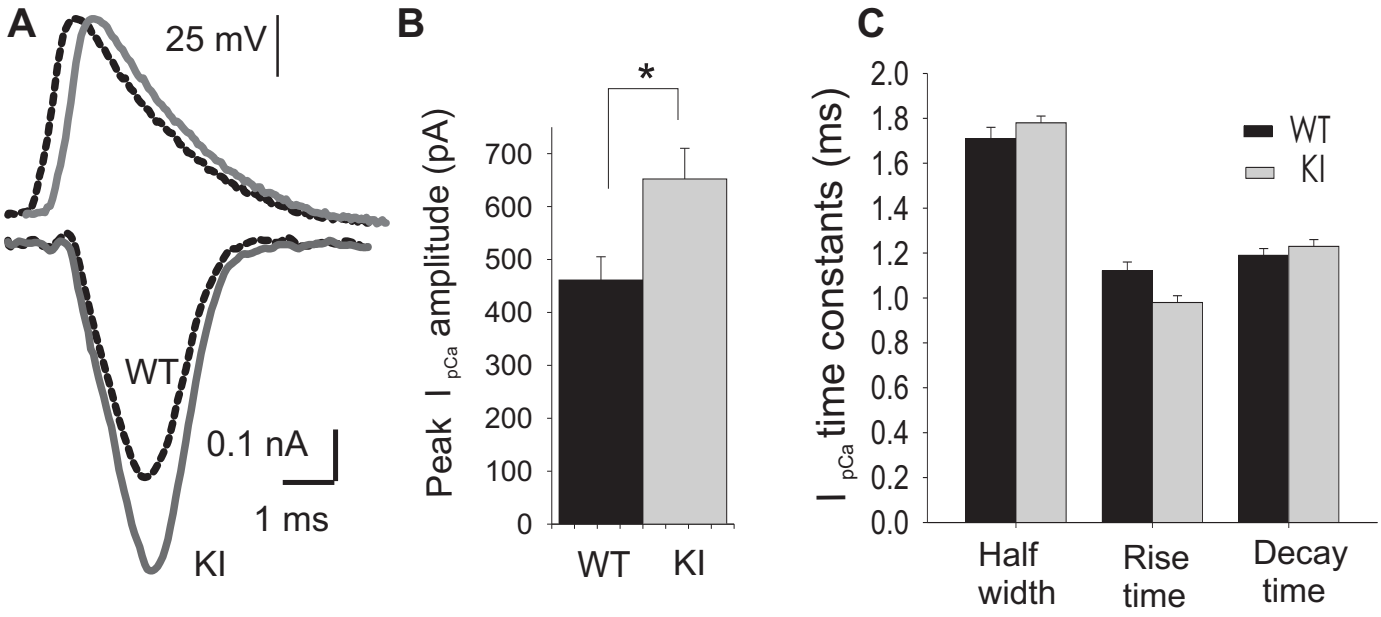

Figure 6